Bias Analysis of Norsar- and ISC-Reported Seismic Event m_b Magnitudes

E. S. HUSEBYE, A. DAHLE, AND K. A. BERTEUSSEN

Norges Teknisk-Naturvitenskapelige Forskningsråd/Norsar
Kjeller, Norway

A skew, approximately log normal, P amplitude distribution across the Norwegian Seismic Array (Norsar) results in a positive bias in its event magnitude estimates. This effect is on the average zeroed out owing to a negative bias caused by signal energy losses during the array beam-forming process. A comparison between Norsar and NOAA magnitudes shows that the difference is largest at $m_b \sim 4.7$ and then tapers off toward both small and large event magnitudes. For NOAA magnitude values less than 4.0, Norsar reports relatively large m_b values. A multivariate analysis of International Seismological Centre (ISC) data for Japan and the Aleutian Islands gave a consistent and linear relationship between the ISC event magnitude and that predicted from subsets of five to nine stations in the $m_b \sim 4.0$–6.0 magnitude range investigated. In this respect the ISC-reported magnitudes are considered unbiased. We also found that the magnitude observations can be approximated by a normal distribution. In many cases the so-called magnitude station correction term was not a constant but a function of event magnitude; i.e., a linear model is recommended for describing the magnitude relationship between individual stations and NOAA, ISC, or 'true' event magnitude. This phenomenon is quantitatively explained as the combined effects of the seismic spectra scaling law (Aki, 1967, 1972) and the frequency-dependent crust–upper mantle transfer function.

When the magnitude parameter is considered as a convenient tool for the ranking of earthquakes, its estimation requires a priori knowledge of the P wave propagation path effects, seismic spectrum scaling laws [*Aki*, 1972], and variations in source mechanism. These topics have interested seismologists for a long time and have resulted in refined and regionalized versions of the *Gutenberg* [1945] magnitude formula given in (1). For examples, see *Gutenberg and Richter* [1956], *Evernden* [1967], *Båth* [1969], *Karnik* [1969], and *Basham and Horner* [1973]. To study this problem, we can formulate a model to characterize the teleseismic P signal amplitude variation over the global seismic network that reports to NOAA and the International Seismological Centre (ISC) or across a large-aperture seismic array like the Norwegian Seismic Array (Norsar). Perturbations or station magnitude corrections are considered due to fixed deterministic variations in earth structure and in that sense are not random. However, it is problematic to predict accurately what station would report an event, and so the final event magnitude can be considered an averaging process on amplitude-period data sampled from a certain probability density distribution. Such an approach in analyzing event magnitude calculations may also be very interesting in the case of an array, as the P amplitude variation is often referred to as intrinsic. In fact, *Ringdal et al.* [1972] found that for the Norsar array the observed P amplitudes could be approximated satisfactorily by a log normal distribution. (A logarithmic transformation of a log normal distribution is normal.)

The topic of this paper is whether a bias (nonrandom errors) exists in the Norsar and ISC m_b parameter estimating procedures. In the Norsar case we would expect a bias in array-calculated magnitudes since a certain amount of wave energy is lost during data processing owing to partially coherent P signals across the array [*Noponen et al.*, 1972]. In the case of the ISC a magnitude bias may occur for very small events since relatively 'high amplitude' stations are intuitively expected to have the best earthquake magnitude reporting performance. A related problem also investigated is whether the regionalized station magnitude correction is a constant or a function of the event magnitude.

Array and Network Magnitude Calculation Procedures

In general, the event magnitude for the ith station is computed according to *Gutenberg*'s [1945] formula, namely,

$$m_i = \log (A_i/T_i) + \log D_i(\Delta, h) + dm_{i,j} \qquad (1)$$

where m_i is the m_b magnitude, A_i is the maximum ground motion short-period P amplitude, T_i is the period, D_i is the distance-depth correction, and $dm_{i,j}$ is the optional station correction for the jth region. The $dm_{i,j}$ parameter is set to zero at Norsar and to our knowledge also in NOAA and ISC network magnitude calculations.

The network m_b body wave magnitude is defined as

$$m_b = \frac{1}{n} \sum_{i=1}^{n} \log (A \cdot D/T), \qquad (2)$$

where n is the number of stations used. Correspondingly, the array m_A magnitude is defined as

$$m_A = \log (A/T)_B + \log D(\Delta, h) \qquad (3)$$

where A_B is the maximum amplitude on the array beam.

For illustrative purposes we can define the beam-forming process as a summation of simple harmonic waves where the signal losses are tied to random timing errors. We can here write for the beam trace $f(t)$ having maximum amplitude A_B (for details see appendix)

$$f(t) = \frac{C_L}{N} \sum_{k=1}^{N} a_k \cos (\omega t) \qquad (4)$$

assuming subarray trace amplitude to be independent of timing errors. Here C_L is a constant denoting signal loss caused by timing errors and/or partial lack of signal coherency during beam forming and N is the number of subarrays. Actually, m_A is estimated in two different ways, the first via the conventional analyst $(A/T)_B$ measurements and the second based on calculation of the kinetic energy of the beam trace P signal. The two procedures give equivalent results, but the second is very convenient for computerized magnitude calculations

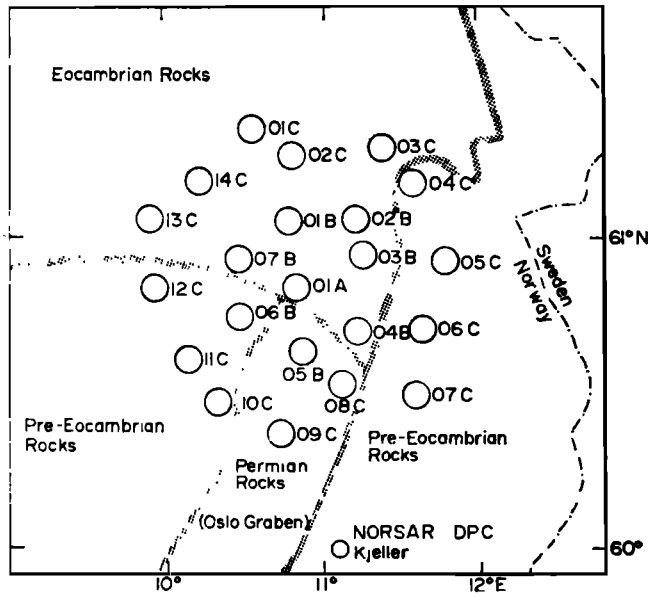

Fig. 1. Norsar array configuration. The geological structures in the siting area are briefly outlined.

[*IBM*, 1967; *Berteussen and Husebye*, 1972]. The above measurements are always performed on original or unfiltered data. To clarify some typical array concepts, we refer to Figure 1, where the Norsar configuration is shown, and to Figure 2, where subarray and array beam traces are shown for two different seismic events. For a detailed software description of the Norsar array, we refer to a paper by *Bungum et al.* [1971].

A brief examination of (2), (3), and (4) shows that unless both the log $(A \cdot D/T)_i$ and a_k terms have symmetric probability density distributions, the calculation procedures represented by these equations are not equivalent. Moreover, if one or both of the above parameters have a skew distribution, the resulting magnitude estimate would be biased. It should be noted that the nonsymmetric log normal amplitude distribution (Figure 3 and Table 1) as observed at Norsar [*Ringdal et al.*, 1972] also quantitatively fits with what is predicted for a so-called random media model for the crust and upper mantle [*Tartarski*, 1961; *Aki*, 1973; *Capon*, 1974].

Possible Nonrandom Errors in Norsar Magnitude m_A Measurements

The standard procedure for m_A measurements is expressed in (3), representing essentially an averaging of subarray amplitudes through the beam-forming operation before the logarithm is taken. Alternatively, m_A could be defined as the average of subarray magnitude measurements in analogy to (2). The difference between the above procedures is that the averaging operation is performed either before or after a log transformation, and thus the amplitude distributions would be different in the two domains. Also remember that signal beam-forming losses occur in the first case but not in the second case. Henceforth the 'correct' method for m_A estimation is according to (2) and thus contrary to standard array routines. The great advantage of the first method is that the amplitude measurements are performed on signals having the best possible signal-to-noise ratio.

The difference between the two magnitude definitions, here denoted m_A and m_{AM} for amplitude and magnitude averaging, respectively, is expressible as

$$dm_{\text{bias}} = m_A - m_{AM} = dm_{\text{loss}} + dm_{\text{skew}} + \text{err} \qquad (5)$$

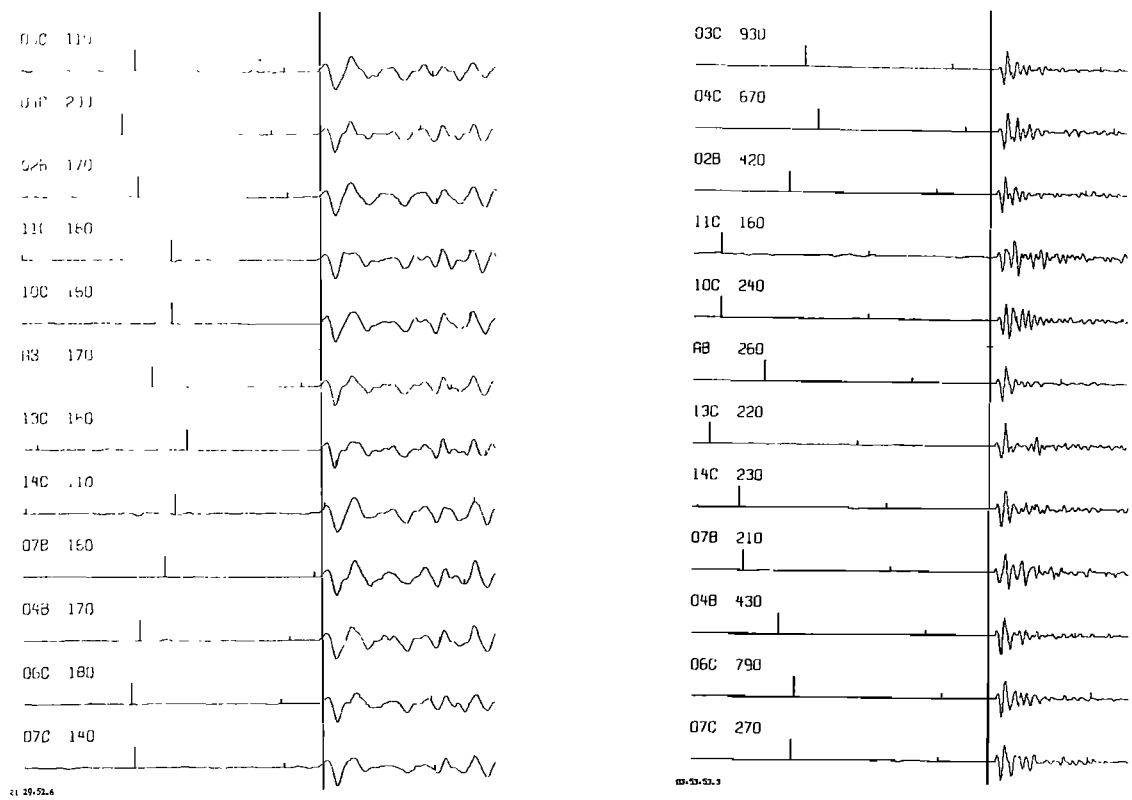

Fig. 2. Display of Norsar array and half of the subarray beam traces for the Colombia and Kazakh events listed in Table 3 as numbers 3 and 14, respectively. The numbers following the subarray codes are amplitude scaling factors. The array beam notation is *AB*, and the time mark unit is 10 s.

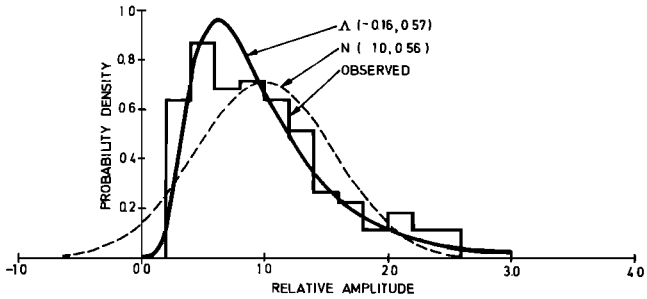

Fig. 3. Observed single-sensor amplitude distribution for a Kamchatka earthquake occurring January 3 at 06h 36m 44s GMT (Norsar bulletin). The amplitude values were measured after applying a 1.0- to 3.4-Hz bandpass filter. The normal and log normal distribution functions estimated from the observed sample mean and variance are also shown.

where dm_{loss} is array beam-forming loss, dm_{skew} is the amplitude skewness effect, and err is an error term having zero mean.

To reject the hypothesis that we have nonrandom errors in m_A requires that the expectation $E(m_A - m_{AM})$ be zero. A possible bias in m_A can tentatively be defined as the difference in magnitude when it is calculated according to (2) and (3), and ignoring the error term, we get

$$dm_{\text{bias}} = \frac{1}{N}\sum_{k=1}^{N} \log a_k - \log A_B \tag{6}$$

where A_B and a_k are maximum amplitudes on the array and subarray traces and N is the number of subarrays. Adding and subtracting the term

$$\log\left(\frac{1}{N}\sum_{k=1}^{N} a_k\right)$$

to (6), we get

$$dm_{\text{bias}} = \log\left(\frac{1}{N}\sum_{k=1}^{N} a_k/A_B\right) + \left(\frac{1}{N}\sum_{k=1}^{N} \log a_k - \log\frac{1}{N}\sum_{k=1}^{N} a_k\right) \tag{7}$$

The first term on the right in (7) is the beam-forming loss, i.e., the log difference between average subarray amplitude and beam trace amplitude as defined in (3). This formulation is an analog to the beam form–spectraform concept of *Lacoss and Kuster* [1970]. The second term expresses the difference due to averaging before and after the log transformation. Thus we can write, using (5),

$$\begin{aligned} dm_{\text{loss}} &= \log\left(\frac{1}{N}\sum_{k=1}^{N} a_k/A_B\right) \\ dm_{\text{skew}} &= \frac{1}{N}\sum_{k=1}^{N} \log a_k - \log\left(\frac{1}{N}\sum_{k=1}^{N} a_k\right) \end{aligned} \tag{8}$$

We are now in a position to test our hypothesis, i.e., whether $E(m_A - m_{AM})$ is zero. The necessary calculations are easy to perform via either (5) or (7) after the required (22 + 1) amplitude measurements have been performed for each Norsar event analyzed. This work is very time consuming, and so in order to ensure a sufficiently large data base, a computerized procedure for magnitude calculations is used. The point here is that earthquake magnitude in principle is tied to the kinetic energy of the P wave through the A/T term in (1). It is then possible to show that the signal power estimate defined in (9), which is equivalent to kinetic energy per unit time and mass, is related to the A/T term in (1) [*IBM*, 1967]:

$$P = \frac{1}{15}\sum_{i=1}^{15} a(i)^2 = \frac{1}{T}\int_0^{T=1.5\,s} a(t)^2 \cdot dt \tag{9}$$

$$P = \pi^2 (A/T)^2 \tag{10}$$

TABLE 1. Subarray Ranking Scores for Different Seismic Regions

	Greece-Turkey	Iran	Kamchatka	Japan	Philippines	South America	Fiji	Average
Subarray Code								
01A	3.8	9.3	8.3	12.2	10.7	6.6	4.4	7.9
01B	9.0	8.5	12.3	7.0	15:3	7.9	11.0	10.1
02B	9.8	5.1	1.3	7.1	18.5	13.9	4.4	8.6
03B	7.0		2.0	16.5	19.2	16.1	8.9	11.6
04B	8.5	12.6	13.6		16.9	12.9	12.9	12.9
05B	11.1	13.6	13.7	17.3	18.2	9.7	7.4	13.0
06B	10.6	4.7		12.0	11.7	4.9	21.6	10.9
07B	7.7	20.4	19.8	4.9	6.2	11.0	4.4	10.6
01C	15.7	17.9	5.4	1.1	3.8		18.9	10.4
02C	11.9	16.2	6.1	2.4	4.1	9.1	14.8	9.2
03C	19.3	16.7	5.3	8.1	3.0	19.2	1.1	10.4
04C	14.6	1.6	10.9	5.2	2.2	7.6	4.8	6.7
05C	15.9	10.2	9.7	2.6	7.6	5.9	17.4	9.9
06C	11.3	20.0	15.9	18.5	19.0	13.2	13.4	15.9
07C	7.7	14.9	19.3	13.0	12.8	17.4	20.5	15.1
08C	10.0	15.8	16.3	17.2	8.9	5.1	11.6	12.1
09C	10.7	7.6	3.3	13.0	21.1	14.0	16.0	12.2
10C	11.5	3.8	16.9	14.1	17.9	12.6	16.8	11.9
11C	13.9	8.0	19.4	13.8	8.0	15.3	14.1	13.2
12C	12.7	6.7	16.0	9.5	12.1	2.5	15.7	10.7
13C	14.9	3.2	5.7	16.3	2.4	10.6	2.1	7.9
14C	15.2	14.0	10.0	19.2	13.4	15.4	10.9	14.0
No. of events	12	14	25	12	15	7	7	
Kendall coefficient concordance	0.31	0.86	0.92	0.84	0.92	0.54	0.98	
X square	77.1	240.8	460.9	201.6	290.5	76.1	129.5	

In all cases the results obtained are significant. For details on the nonparametric rank test, see *Siegel* [1956].

TABLE 2. Estimated Magnitude Biases Due to Subarray Power Loss and Skewed Maximum Power Distribution, Conditioned on Number of Subarrays (This Parameter Represents a Decreasing Order of Subarrays Based on Maximum Power Ranking)

No. of Subarrays	dm_{loss}, m_b units	dm_{skew}, m_b units
3	0.28 ± 0.06	0.0 ± 0.01
6	0.23 ± 0.05	-0.01 ± 0.01
9	0.20 ± 0.04	-0.02 ± 0.01
12	0.16 ± 0.04	-0.03 ± 0.02
15	0.14 ± 0.04	-0.04 ± 0.02
18	0.11 ± 0.03	-0.05 ± 0.03
Operational 19 ≤ no. ≤ 22	0.08 ± 0.03	-0.07 ± 0.03

Estimated skewness of subarray maximum power distribution is 1.26 ± 0.63.

Estimated skewness for log transformation of maximum power is -0.10 ± 0.42; correlation between signal loss and skewness effects, -0.40 correlation unit; sample size, 222 events.

The window length used for power P estimation is somewhat arbitrarily set to 1.5 s, but *Berteussen and Husebye* [1972] found no significant difference in magnitude estimates based on $A_{B_{max}}$ and $P_{B_{max}}$ measurements and those using (3). As was mentioned before, unfiltered data are used when event magnitudes are estimated.

A large number of Norsar-recorded events occurring from April to December 1972 were subjected to m_A and m_{AM} magnitude measurements using the definitions in (6), (8), (9), and (10). The power estimates are corrected for noise on both the subarray and the array beam level. The event selection criteria were good signal-to-noise ratio, epicentral distance range 35°–95°, and beam losses less than 6 dB or 0.3 magnitude unit. The second restriction removes events characterized by complicated signals due to upper mantle inhomogeneities, and the third criterion rejects events grossly mislocated and explosions or explosionlike earthquakes in central Asia having dominant periods around 0.4–0.6 s. Altogether, 222 events were analyzed, and the final results are presented in Table 2. For a few events, dm_{skew} and dm_{loss} values are listed in Table 3. Case study results for the events displayed in Figure 2 are presented in Table 4. The relatively long period, highly correlated signal traces of the Colombia event and the very short period, somewhat dissimilar subarray signals of the eastern Kazakh event represent extremities in our m_A analysis. In Tables 2 and 4, dm_{loss} and dm_{skew} are tabulated as a function of the number of subarrays. The second parameter represents a successive signal summation from a decreasing ordering of subarrays based on maximum signal power ranking. As was expected from the approximately log normal a_k distribution and the independence between signal shape and signal amplitude (appendix), we got relatively large dm_{loss} values when the number of subarrays was small. On the other hand, the skewness effect is not easily observable before the number of subarrays becomes sufficiently large. As $E(dm_{bias}) = E(dm_{loss}) + E(dm_{skew})$, we infer that there exists a bias of about 0.01 magnitude unit in the Norsar magnitude estimate. As can also be seen from Table 2, the log transformation of power results in a negative skewness, however small, in absolute value in comparison with the skewness of the untransformed distribution. Accordingly, this effect has been overestimated by an amount less than 10%.

As a consequence of the results presented, we cannot reject the hypothesis that nonrandom errors exist in the magnitude estimate as reported by the Norsar array. However, this small bias can be ignored safely in comparison with random errors contributing to the total magnitude estimate uncertainty. The exceptions are, as was pointed out above, local earthquakes and extremely short periodic events. In the latter cases, averaging of subarray magnitude estimates gives the best results.

Possible loss and skewness effects during subarray beam forming have been neglected in the magnitude measurements discussed so far. Analysis of nine earthquakes indicates that the single sensor–subarray beam relationship represents a miniature of the relationship between subarray and array beam traces. That is, small signal losses [*Noponen et al.*, 1972] are compensated for by a small skewness in the sensor amplitude distribution.

So far, our Norsar m_b bias analysis has been restricted solely to the computational procedures and structural effects typical of the array itself. Another possible bias source is the

TABLE 3. Biased Errors Due to Array Beam-Forming Power Loss and Skewed Subarray Maximum Power Distribution for a Subsample of the 222 Events Analyzed

Event	Date, 1972	Origin Time	Region	m_b (Norsar)	Period, s	Maximum Power Skewness	dm_{loss}, m_b units	dm_{skew}, m_b units
1	Sep. 19	04h 07m 41.2s	Ryukyu Islands	5.2	0.5	1.62	0.14	-0.17
2	Sep. 30	10h 37m 03.5s	Afghanistan-USSR border	5.1	0.6	2.47	0.11	-0.13
3	Aug. 26	03h 54m 15.4s	Eastern Kazakh	5.3	0.7	1.75	0.19	-0.17
4	Oct. 13	05h 12m 58.8s	Kashmir	5.2	0.7	1.53	0.08	-0.09
5	Oct. 14	00h 10m 30.2s	Kurile Islands	5.6	0.7	2.00	0.08	-0.08
6	Dec. 7	23h 49m 31.8s	Honshu, Japan	4.9	0.7	2.06	0.11	-0.10
7	Aug. 26	11h 48m 57.6s	Aleutian Islands	4.5	0.8	1.02	0.14	-0.08
8	Sep. 25	16h 11m 47.6s	Honshu, Japan	4.8	0.8	2.62	0.12	-0.14
9	Aug. 28	14h 37m 28.3s	Philippine Islands	5.4	1.0	1.09	0.06	-0.06
10	Sep. 22	20h 09m 33.6s	Taiwan	5.6	1.0	0.49	0.04	-0.02
11	Oct. 29	07h 31m 54.9s	Honshu, Japan	5.6	1.1	1.87	0.10	-0.08
12	Oct. 29	03h 19m 55.5s	North Atlantic	4.7	1.2	0.93	0.09	-0.04
13	Dec. 8	18h 26m 07.2s	S. Sumatra	5.4	1.2	1.53	0.04	-0.04
14	Sep. 17	21h 30m 11.3s	Colombia	5.4	1.3	0.44	0.03	-0.02
15	Dec. 6	05h 44m 06.0s	Mid-Indian rise	5.7	1.3	1.11	0.11	-0.04
16	Dec. 9	06h 54m 49.1s	North Atlantic	5.3	1.3	1.66	0.10	-0.03
17	Aug. 31	02h 36m 30.0s	Central America	4.9	1.4	1.18	0.04	-0.03

All available subarrays were used in the calculations.

dm_{ij} station correction term in (1), and this problem is the topic of the next section.

NORSAR m_b MAGNITUDES VERSUS THOSE OF NOAA

As is well known, P signal amplitudes vary considerably from one station to another and also as a function of seismic region, this variation necessitating the correction term dm_{ij} in (1). For seismographs having widely different transfer functions, say, short-period Benioffs in comparison with the more broad-band Kirnos instruments, the scaling law of seismic spectrum [*Aki*, 1972] is likely to play an important role. Here the crust–upper mantle transfer function remains fixed, whereas the frequency content of the incoming signals may vary according to the seismic spectrum scaling law. The significance of this factor has been much discussed [*Davies*, 1968] and recently demonstrated by *Marshall et al.* [1972], who reported nonrandom differences in m_b magnitudes measured on high- and low-pass-filtered outputs from a broad-band instrument. Similar effects may be observable even for m_b measurements restricted to narrow-band instruments owing to strong frequency dependence of the crust-mantle transfer function. We will return to this problem in a later section.

In comparing Norsar and NOAA estimated magnitudes for the jth region, we have used a simple linear model as given below:

$$m_{Aj} = \alpha_j m_j + \beta_j + \epsilon_{Aj} \tag{11}$$

where m_A is the Norsar array magnitude, m is the NOAA m_b magnitude, and ϵ_{Aj} is an error term. The reason for choosing a magnitude model given by (11) is that from the above discussion we cannot exclude the possibility of magnitude dependency of the regionalized station correction term dm_{ij} in (1). The possibility that the dm_{ij} term in (1) is a constant, corresponding to the standard model for regionalized station magnitude corrections, is included in (11), i.e., equivalent to $\alpha_j = 1.0$. To differentiate between these two models is simply to check whether α_j is significantly different from 1.0.

The data used are taken from NOAA and Norsar bulletins and cover the period from February to September 1972. The NOAA magnitude is considered the best available estimate of the event magnitude. Moreover, the m_A data are assumed to be sampled independently of those of NOAA, as the latter organization seldom uses Norsar data owing to array bulletin editing delays. The events finally used in analysis are restricted such that Norsar location errors are less than 8° in distance and azimuth and the maximum m-m_A difference permitted is 1.0 magnitude unit. It is worth noting that the D_i correction in (1) is tied to the Norsar epicenter solution. The distance difference between the Norsar and NOAA solutions for 1191 teleseismic events was found to be -30 ± 292 km [*Bungum and Husebye*, 1974]. The corresponding random error in the D_i term would be less than approximately ± 0.03 magnitude unit, which is considered insignificant. Moreover, the A/T parameter in (1) is always tied to the Norsar epicenter solution.

TABLE 4. Loss and Skewness Biases Conditioned on Number of Subarrays for Events 3 and 14 in Table 3

No. of Subarrays	Colombia		Eastern Kazakh	
	dm_{loss}	dm_{skew}	dm_{loss}	dm_{skew}
3	0.15	0.0	0.49	0.0
6	0.12	0.0	0.41	-0.03
9	0.11	0.0	0.36	-0.05
12	0.09	-0.01	0.31	-0.07
15	0.07	-0.01	0.27	-0.09
18	0.05	-0.01	0.24	-0.12
Operational $19 \leq$ no. ≤ 22	0.03	-0.02	0.19	-0.17

The results obtained are listed as a function of different regions and displayed in Table 5 and Figure 4. Obviously, the functional relationship between Norsar and NOAA magnitudes is not a constant and, as expected, varies somewhat with individual seismic regions. Initially, higher-order polynomials (maximum of fourth order) were fitted to the m-m_A data base, but analysis of the sum of the squares of deviations from regression showed that quadric and higher-order effects, when they were isolated, were small in com-

TABLE 5. Regression Coefficients and Standard Error $\sigma(a)$ for a Simple Linear Relationship (Equation (11)) Between NOAA and Norsar Event Magnitudes

Region No.	Region*	Regression Coefficient		No. of Events	Minimum m_b
		$a \pm \sigma(a)$	b		
1	Alaska-Aleutians	0.88 ± 0.053†	0.34	132	3.7
2	Mexico-Central America	0.80 ± 0.066†	0.74	119	3.5
3	Kermadec-Fiji	0.78 ± 0.089†	0.87	97	3.6
4	New Hebrides-Solomon	0.68 ± 0.070†	1.30	113	3.8
5	Guam-Japan	0.84 ± 0.055†	0.70	115	3.8
6	Japan-Kurile-Kamchatka	0.86 ± 0.043†	0.58	205	3.6
7	Taiwan	0.88 ± 0.113	0.29	47	4.0
8	Philippines	1.10 ± 0.160	-0.61	68	4.3
9	Indonesia	1.03 ± 0.146	-0.32	45	4.8
10	India-China	1.13 ± 0.080	-0.95	67	4.2
11	Western Asia	0.78 ± 0.068†	0.87	63	3.9
12	Middle East	0.83 ± 0.100	0.35	57	3.6
13	Hindu Kush	0.87 ± 0.087	0.69	64	3.3
14	Local	0.90 ± 0.061	0.20	120	3.6
15	Teleseismic	0.86 ± 0.023†	0.50	853	3.3
16	Core	0.72 ± 0.055†	1.15	210	3.6

*Local events comprise regions 11 and 12; core events, regions 3 and 4; teleseismic events, regions 1, 2, 5 to 10, and 13.
†Regression coefficients significantly different from 1.0 at the 5% level.

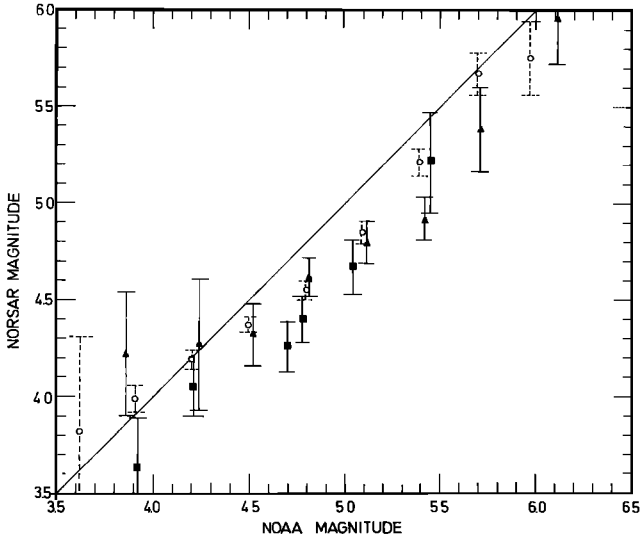

Fig. 4. Plot of Norsar-NOAA data for the Japan-Kurile-Kamchatka region. Group averages, including 0.95 confidence limits for local (solid squares), teleseismic (solid triangles), and core (open circles) events (see Table 5), are shown. The thin line is a reference for identical Norsar-NOAA magnitudes.

parison with the dominant linear term. In short, (11) gave the best fit to the observational data.

Some attention should be given to the problem of differentiating between prognosis and physical models. An example of the former is (11), in which it is asked what the expected Norsar event magnitude is, given the NOAA event magnitude. If α_j is significantly different from 1.0, a linear model gives a better functional relationship between the Norsar and NOAA reported event magnitudes than the standard model where α_j is assumed to be 1.0. It is worth noting in this section that (11) is interpreted as a prognosis model. On the other hand, if (11) is taken to represent a physical model, the NOAA magnitude is interpreted as an estimate of the true event m_b value. Then the occurrence of random observational errors in the NOAA m_b estimate would result in a negative bias in the estimated regression coefficient a_j, namely,

$$E(a_i) \approx \frac{\alpha_i \cdot \sigma^2(m_i)}{\sigma^2(m_i) + \sigma^2(dm_i)} \qquad (12)$$

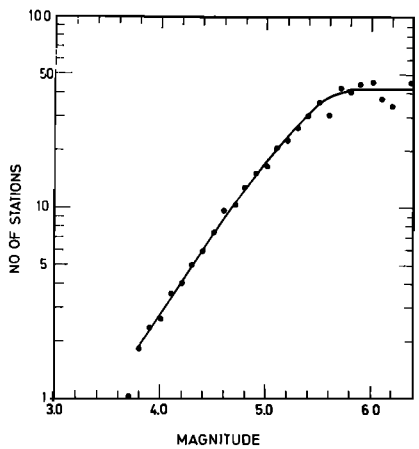

Fig. 5. Average number of stations in the global network reporting earthquakes occurring in the Japan region during 1968 as function of ISC-reported magnitude. Large scattering was observed in the data taken from ISC bulletin files.

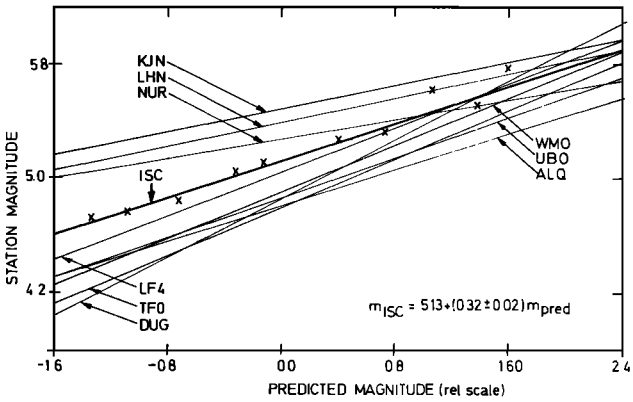

Fig. 6. A comparison between event magnitudes as predicted from a multivariate analysis of ISC data for Japan and those of the individual stations used in the analysis. The relationship between ISC-reported magnitudes and predicted magnitude is also given. The crosses are observed points for this line. This figure is based on 40 events occurring in the Japan region in 1968 and reported jointly by the nine stations listed on the figure. See also Table 6.

where α_j is the correct regression coefficient, m_j is the true magnitude, and dm_j is the observational error for the jth region. Thus if (11) is interpreted as a physical model, we cannot conclude that α_j is significantly different from 1.0 since we do not know if the $\sigma^2(dm_j)$ term could be ignored. However, we have tried to resolve this problem in a later section by using ISC magnitude data and a different analysis procedure.

The above results do not necessarily imply that a linear model gives the best functional relationship between NOAA and Norsar event magnitude estimates. In fact, grouping and averaging the data in a number of NOAA magnitude intervals of 0.3 unit in width (Figure 4) seem to give a slightly better fit between the m and m_A data. Figure 4 shows that the maximum difference between m and m_A occurs at magnitudes around $m \sim 4.7$ and then tapers off toward higher and lower event magnitudes. Such a model should be kept in mind when the results of the linear regression analysis presented in Table 5 are interpreted. This may explain why we got negative intercept values for regions 8, 9, and 10, where the data were restricted to relatively large events (i.e., m magnitude values larger than around 4.2 units).

An interesting aspect of the observed NOAA-Norsar magnitude variation is that for very small events, say, $m \leq 4.0$, Norsar in general reports magnitude values that are too large in comparison with those of NOAA. This point is of considerable importance when event detectabilities of

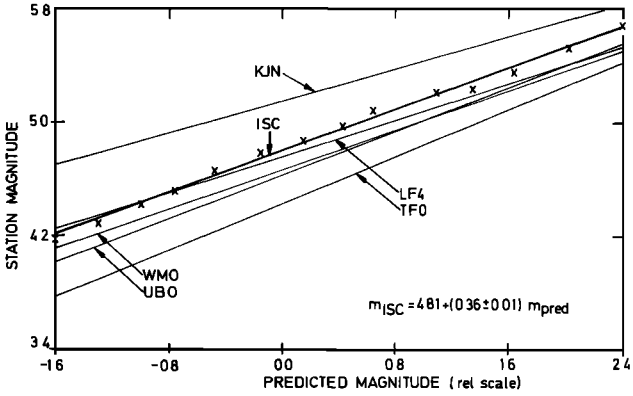

Fig. 7. Same as Figure 6 for 219 events occurring in the Japan region in 1968 and reported jointly by five stations. See also Table 7.

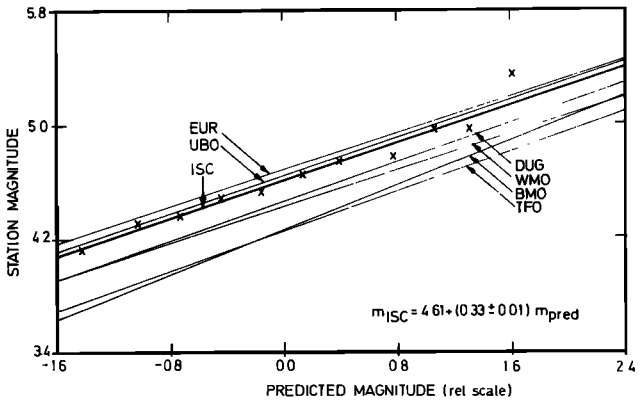

Fig. 8. Same as Figure 6 for 129 events occurring in the Aleutian region in the interval 1966–1969 and reported jointly by six stations. See also Table 8.

networks, seismic arrays, etc. are investigated. However, it is beyond the scope of this paper to discuss further the implications of these results.

ISC Event Magnitude Estimate

So far we have considered the functional relationship between NOAA and Norsar magnitude estimates and mostly ignored the physical explanation of the observations. Before commenting further on this subject, we have to check whether the m_b magnitude as reported by the ISC (corresponding NOAA data on tape for single stations are not available) is a good estimate of the true magnitude and whether the dm_{ij} term in (1) can be considered a function of magnitude also for ordinary seismic stations. In order to test the above hypothesis, an analysis was undertaken of ISC-reported events in 1968 in the Japan region and in the interval 1966–1969 for the Aleutian Island region. The Japan and Aleutian regions are defined as 32°–48°N, 130°–147°E and 48°–58°N, 167°E–160°W, respectively. In general, this kind of data is difficult to handle owing to the variability in the individual stations' event magnitude reporting performances as indicated in Figure 5.

The first step was a probability density distribution check on the normality of the AD/T parameter in (1) using the Smirnov-Kolmogorov test procedure. For events of magnitude $m \geq 5.2$ the data passed the test at the 0.10 level but not for small events. In the latter case the reason was that very few, and mostly the same, stations detect small events, data redundancy thus being caused in the subsampling procedure. The next step was an analysis of 40 and 219 events in Japan recorded jointly by a set of nine and five stations and 129 Aleutian Island events recorded jointly by six stations. Conceptually, the following multivariate model is used:

$$Y_{ij} = \beta_j + \alpha_j m_i + \epsilon_{ij} \qquad (13)$$

where Y_{ij} is the observed magnitude of the ith event at the jth station, α_j and β_j are unknown parameters referring to the jth station, m_i is the true or correct but unknown event magnitude, and ϵ_{ij} is the residual. Contrary to the earlier case when a prognosis model was used in analysis of the Norsar-NOAA relationship, this time we consider a linear physical model as expressed in (13). The above formulation corresponds to the usual one-component model with m_i as the component [e.g., *Anderson*, 1958]. In this model we must impose some restriction in order to obtain uniqueness of the parameters α_j, β_j, and m_i.

TABLE 6. Predicted Magnitude, ISC-Reported Magnitude, and Station Magnitude Averaged Within Nine Intervals

Number of Observations	Predicted Magnitude	ISC-Reported Magnitude	LHN	LF4	UBO	TFO	WMO	KJN	NUR	ALQ	DUG
1	1.60	5.78	6.10	5.70	4.90	5.60	5.70	6.00	5.60	5.10	5.70
6	1.38 ± 0.09	5.52 ± 0.11	5.63 ± 0.22	5.62 ± 0.08	5.25 ± 0.35	5.35 ± 0.16	5.52 ± 0.12	5.72 ± 0.16	5.45 ± 0.21	5.43 ± 0.12	5.55 ± 0.29
2	1.06 ± 0.14	5.63 ± 0.12	5.80 ± 0.14	5.40 ± 0.0	5.40 ± 0.0	5.20 ± 0.0	5.15 ± 0.07	5.80 ± 0.42	5.60 ± 0.14	5.15 ± 0.07	5.35 ± 0.07
6	0.73 ± 0.10	5.33 ± 0.10	5.48 ± 0.38	5.38 ± 0.13	5.12 ± 0.13	5.00 ± 0.09	5.27 ± 0.14	5.60 ± 0.35	5.42 ± 0.28	5.00 ± 0.17	5.28 ± 0.10
4	0.39 ± 0.08	5.27 ± 0.14	5.47 ± 0.15	5.05 ± 0.26	5.27 ± 0.25	4.97 ± 0.22	5.05 ± 0.21	5.60 ± 0.18	5.35 ± 0.10	4.67 ± 0.21	5.07 ± 0.13
2	-0.13 ± 0.18	5.12 ± 0.13	5.30 ± 0.14	5.20 ± 0.0	4.85 ± 0.07	4.55 ± 0.21	4.90 ± 0.21	5.45 ± 0.35	5.20 ± 0.14	4.85 ± 0.21	4.70 ± 0.14
2	-0.33 ± 0.03	5.06 ± 0.23	5.40 ± 0.0	4.95 ± 0.07	4.80 ± 0.0	4.50 ± 0.14	4.85 ± 0.07	5.50 ± 0.0	5.25 ± 0.07	4.55 ± 0.07	4.65 ± 0.07
8	-0.73 ± 0.08	4.85 ± 0.13	5.29 ± 0.27	4.77 ± 0.18	4.74 ± 0.13	4.29 ± 0.12	4.52 ± 0.07	5.26 ± 0.28	5.09 ± 0.20	4.62 ± 0.42	4.55 ± 0.11
3	-1.08 ± 0.04	4.77 ± 0.02	5.07 ± 0.15	4.57 ± 0.12	4.53 ± 0.06	4.27 ± 0.06	4.50 ± 0.10	5.20 ± 0.26	5.17 ± 0.25	4.40 ± 0.10	4.33 ± 0.06
6	-1.34 ± 0.15	4.72 ± 0.11	5.15 ± 0.08	4.55 ± 0.26	4.17 ± 0.18	4.08 ± 0.25	4.43 ± 0.08	5.33 ± 0.14	5.07 ± 0.10	4.52 ± 0.13	4.12 ± 0.15

Each interval 0.3 predicted magnitude unit in width. Data base is 40 events occurring in Japan region in 1968 and reported jointly by nine stations used. LHN, Lillehammer, Norway; LF4, Lasa F ring; UBO, Uinta basin, Utah; TFO, Tonto Forest, Arizona; WMO, Wichita Mountains, Oklahoma; KJN, Kajaani, Finland; NUR, Nurmijarvi, Finland; ALQ, Albuquerque, New Mexico; DUG, Dugway, Utah.

TABLE 7. Predicted Magnitude, ISC-Reported Magnitude, and Station Magnitude Averaged Within 14 Intervals

Number of Observations	Predicted Magnitude	ISC-Reported Magnitude	LF4	UBO	TFO	WMO	KJN
7	2.41 ± 0.13	5.65 ± 0.16	5.24 ± 0.46	5.60 ± 0.38	5.49 ± 0.13	5.57 ± 0.16	5.96 ± 0.15
8	2.02 ± 0.12	5.52 ± 0.13	5.50 ± 0.17	5.29 ± 0.33	5.24 ± 0.20	5.45 ± 0.15	5.74 ± 0.24
10	1.64 ± 0.10	5.35 ± 0.11	5.36 ± 0.26	5.32 ± 0.12	5.04 ± 0.14	5.27 ± 0.13	5.53 ± 0.30
9	1.35 ± 0.09	5.24 ± 0.14	5.18 ± 0.21	5.19 ± 0.16	5.02 ± 0.15	5.10 ± 0.07	5.51 ± 0.38
12	1.09 ± 0.07	5.21 ± 0.13	5.12 ± 0.11	4.93 ± 0.31	5.00 ± 0.15	5.07 ± 0.17	5.42 ± 0.29
8	0.64 ± 0.06	5.09 ± 0.16	5.07 ± 0.22	4.76 ± 0.23	4.77 ± 0.27	4.76 ± 0.16	5.42 ± 0.36
17	0.42 ± 0.09	4.98 ± 0.17	4.96 ± 0.18	4.81 ± 0.21	4.55 ± 0.17	4.79 ± 0.15	5.28 ± 0.35
17	0.14 ± 0.08	4.87 ± 0.11	4.87 ± 0.19	4.76 ± 0.16	4.44 ± 0.17	4.68 ± 0.11	5.14 ± 0.26
28	-0.16 ± 0.08	4.79 ± 0.12	4.76 ± 0.18	4.61 ± 0.22	4.34 ± 0.14	4.56 ± 0.13	5.09 ± 0.25
31	-0.48 ± 0.09	4.66 ± 0.12	4.59 ± 0.17	4.46 ± 0.13	4.21 ± 0.17	4.51 ± 0.18	5.05 ± 0.25
29	-0.76 ± 0.08	4.51 ± 0.11	4.48 ± 0.17	4.32 ± 0.16	4.16 ± 0.18	4.41 ± 0.13	4.93 ± 0.22
31	-1.00 ± 0.09	4.43 ± 0.13	4.43 ± 0.18	4.19 ± 0.29	4.04 ± 0.15	4.37 ± 0.14	4.86 ± 0.22
9	-1.29 ± 0.08	4.29 ± 0.10	4.37 ± 0.12	4.14 ± 0.22	3.90 ± 0.17	4.19 ± 0.13	4.78 ± 0.20
3	-1.62 ± 0.12	4.18 ± 0.15	4.10 ± 0.20	4.03 ± 0.25	3.77 ± 0.25	4.20 ± 0.10	4.70 ± 0.20

Each interval 0.3 predicted magnitude unit in width. Data base is 219 events occurring in Japan region in 1968 and reported jointly by five stations used.

LF4, Lasa F ring; UBO, Uinta basin, Utah; TFO, Tonto Forest, Arizona; WMO, Wichita Mountains, Oklahoma; KJN, Kajaani, Finland.

Adding a constant c_1 to the magnitude m_i in (13) and subtracting $\alpha_j c_1$ from the β_j term give

$$Y_{ij} = \beta_j - \alpha_j c_1 + \alpha_j(m_i + c_1) + \epsilon_{ij} \quad (14)$$

Multiplying m_i in (13) by a constant c_2 gives

$$Y_{ij} = \beta_j + (\alpha_j/c_2)(m_i \cdot c_2) + \epsilon_{ij} \quad (15)$$

Combining (14) and (15), we get

$$Y_{ij} = \beta_j - (\alpha_j/c_2)(c_1 \cdot c_2) + (\alpha_j/c_2)(m_i + c_1)\cdot c_2 + \epsilon_{ij} \quad (16)$$

where c_1 and c_2 can be chosen arbitrarily. Equation (16) can be rewritten as

$$Y_{ij} = \beta_j^* + \alpha_j^* m_i^* + \epsilon_{ij} \quad (17)$$

where $\beta_j^* = \beta_j - (\alpha_j \cdot c_1)$, $\alpha_j^* = \alpha_j/c_2$, and $m_i^* = (m_i + c_1)\cdot c_2$. We have here chosen c_1 and c_2 so that

$$\frac{1}{N}\sum_{i=1}^{N} m_i^* = 0 \qquad \sum_{j=1}^{M} \alpha_j^{*2} = 1$$

To estimate the unknowns, the method of least squares is used; i.e., we minimize

$$\sum_{i=1}^{N}\sum_{j=1}^{M}(Y_{ij} - \beta_j^* - \alpha_j^* m_i^*)^2 = \sum_{i=1}^{N}\sum_{j=1}^{M}\epsilon_{ij}^2 \quad (18)$$

where N is the number of events and M is the number of stations. Thus in the above component model the true magnitude can be estimated, except for the location and the scale units c_1 and c_2. In other words, a possible bias in the ISC-reported event magnitudes requires a nonlinear relationship between the former parameter and the event magnitudes determined from the M stations in the above component model.

An additional benefit of this analysis procedure is that we can actually test whether a linear model ($\alpha_j \neq 1.0$ in (13)) or the standard model $\alpha_j = 1.0$ should be used in analyzing the physical relationship between true event magnitude and m_b values reported by an individual station. One way is to check if the regression coefficients α_j or α_j^* are significantly different from each other. Following *Morrison* [1967], we used the following asymptotic test of the hypothesis:

$$H_0: \alpha_j^* = \alpha_{j0}^* \quad (19)$$

where $\alpha_{j0}^* = 1/M^{1/2}$ for $j = 1, \cdots, M$.

The test statistic

$$\chi^2 = (N - 1)[l\alpha_{j0}^* S^{-1}\alpha_{j0}^* + (1/l)\alpha_{j0}^{*1} S\alpha_{j0}^* - 2] \quad (20)$$

is approximately distributed as a chi-squared variate with $M - 1$ degrees of freedom when H_0 is true. In (20), l is the largest eigenvalue obtained in the solution of (18), S is the covariance matrix, α_{j0}^{*1} is the transpose of the α_{j0}^* vector, and S^{-1} is the matrix inverse.

The results obtained are displayed in Figures 6, 7, and 8 for the nine-station–40 event (Japan), five-station–219 event (Japan), and six-station–129 event combinations. In Tables 6, 7, and 8 some of the original ISC data used are listed (i.e., the average ISC and individual station m_b magnitude calculated in 0.3-unit intervals of the predicted event magnitude). Only the ISC m_b data in Tables 6–8 are included in Figures 6–8 to avoid confusing figures, but the individual station magnitude values exhibit a very similar pattern if they are plotted. The seismic station coordinates are given in Table 9.

The above results of the multivariate analysis of the ISC data for the Japan region show quite clearly that the magnitude correction factor for some seismic stations linearly decreases with increasing magnitude. Actually, the H_0 hypothesis discussed above had to be rejected at the 0.01 level; i.e., the α_j^* regression coefficients are significantly different from each other. For the Aleutian Island region, where the data base is restricted to North American stations, the dm_{ij} corrections seem to be constants (i.e., independent of event magnitude) since the H_0 hypothesis could not be rejected. As a consequence of the above results and also of those obtained in the Norsar-NOAA data analysis, it is recommended that a linear model be used in studies involving magnitude station corrections. In many cases this model gives a better fit to the observational data than the standard model (dm_{ij} constant in (1)); besides, the standard model is included in the linear model.

The ISC-reported event magnitudes for the Japan and

TABLE 8. Predicted Magnitude, ISC-Reported Magnitude, and Station Magnitude Averaged Within 12 Intervals

Number of Observations	Predicted Magnitude	ISC-Reported Magnitude	UBO	TFO	BMO	EUR	WMO	DUG
6	2.83 ± 0.38	5.50 ± 0.14	5.50 ± 0.21	5.43 ± 0.40	5.37 ± 0.30	5.37 ± 0.40	5.48 ± 0.31	5.35 ± 0.34
4	1.61 ± 0.21	5.35 ± 0.35	5.20 ± 0.23	4.80 ± 0.24	4.85 ± 0.17	5.17 ± 0.36	4.92 ± 0.26	5.10 ± 0.08
7	1.32 ± 0.05	4.97 ± 0.10	5.03 ± 0.34	4.80 ± 0.24	4.73 ± 0.20	5.23 ± 0.16	4.71 ± 0.27	4.94 ± 0.15
7	1.07 ± 0.09	4.97 ± 0.16	4.99 ± 0.23	4.66 ± 0.14	4.66 ± 0.13	5.03 ± 0.29	4.79 ± 0.21	4.81 ± 0.15
6	0.78 ± 0.11	4.88 ± 0.15	5.00 ± 0.14	4.50 ± 0.38	4.43 ± 0.12	5.03 ± 0.27	4.60 ± 0.17	4.78 ± 0.17
6	0.40 ± 0.07	4.74 ± 0.14	4.78 ± 0.19	4.43 ± 0.12	4.28 ± 0.17	4.88 ± 0.17	4.55 ± 0.24	4.63 ± 0.12
19	0.14 ± 0.09	4.65 ± 0.19	4.71 ± 0.17	4.27 ± 0.18	4.26 ± 0.13	4.76 ± 0.19	4.46 ± 0.20	4.58 ± 0.20
13	-0.15 ± 0.07	4.53 ± 0.13	4.67 ± 0.19	4.18 ± 0.22	4.18 ± 0.18	4.58 ± 0.27	4.35 ± 0.13	4.47 ± 0.12
17	-0.43 ± 0.09	4.49 ± 0.17	4.54 ± 0.17	4.12 ± 0.19	4.06 ± 0.15	4.69 ± 0.25	4.23 ± 0.16	4.22 ± 0.10
22	-0.73 ± 0.09	4.36 ± 0.16	4.36 ± 0.20	3.98 ± 0.17	4.01 ± 0.18	4.45 ± 0.31	4.26 ± 0.14	4.21 ± 0.14
17	-1.02 ± 0.07	4.31 ± 0.17	4.31 ± 0.12	3.89 ± 0.11	3.99 ± 0.14	4.23 ± 0.19	4.11 ± 0.18	4.11 ± 0.17
5	-1.42 ± 0.13	4.12 ± 0.06	4.04 ± 0.22	3.76 ± 0.09	3.78 ± 0.08	4.12 ± 0.28	4.04 ± 0.05	4.10 ± 0.19

Each interval 0.3 predicted magnitude unit in width. Data base is 129 events occurring in the Aleutian Island region from 1966 to 1969 and reported jointly by six stations. UBO, Uinta basin, Utah; TFO, Tonto Forest, Arizona; BMO, Blue Mountains, Oregon; EUR, Eureka, Nevada; WMO, Wichita Mountains, Oklahoma; DUG, Dugway, Utah.

Aleutian regions, with respect to those predicted from a subset of stations, vary consistently and linearly as a function of magnitude. In Figures 6 and 8 the fit between ISC-reported and predicted magnitudes is slightly unsatisfactory at large m_b values, but few observational data were available in this range. From these results we conclude that the ISC-reported m_b values are unbiased in the magnitude range considered.

DISCUSSION

In the analysis of Norsar and ISC magnitude data we have forwarded a model, namely, a log normal probability density distribution, to characterize the teleseismic P wave amplitude period variation across an array or the global seismological network. This hypothesis, which is based on Kolmogorov-Smirnov tests of significance of observational data, can be explained in terms of either a random media model for crust and upper mantle structures [e.g., *Tartarski,* 1961] or the response of a multilayered earth as forwarded by *Ringdal et al.* [1972]. In this respect, Norsar can be considered a miniature of the global network since we found that the P wave amplitude variation across Norsar can be approximated by a log normal distribution. From this point of view the event magnitude estimation, as defined in (2) and used by ISC and NOAA, can be considered a problem of determining a reliable and unbiased first-moment estimate of data samples selected, not necessarily randomly, from a population that is at least approximately normally distributed. To put it otherwise, for large events the average of observed station m_b values would give the best estimate of the true event magnitude. This statement is not necessarily valid for small events when the data base is restricted to magnitude measurements by a few and often the same stations. In the special case of Norsar the event magnitude is measured on the beam trace, but the amplitude skewness effect is compensated for by signal losses due to small random timing errors and signal incoherency.

In the above discussion the observed station magnitude corrections are considered a sampling effect. For example, Tables 6 and 8 show that five out of nine and three out of six stations most frequently reporting events from the Japan and Aleutian regions, respectively, have a negative magnitude station correction with respect to ISC. Typically, a relatively large number of sensitive stations that often have negative dm_{ij} values are located in North America. In short, since

TABLE 9. Stations Used in Analysis of ISC Data

Station	Location	Latitude	Longitude
ALQ	New Mexico	34.9°N	106.5°W
BMO*	Oregon	44.8°N	117.3°W
DUG	Utah	40.2°N	112.8°W
EUR	Nevada	32.5°N	116.0°W
KJN	Finland	64.1°N	27.7°E
LF4*	Lasa, Montana	47.4°N	106.9°W
LHN*	Norway	61.0°N	10.9°E
NAO*	Norsar, Norway	60.8°N	10.8°E
NUR	Finland	60.5°N	24.6°E
TFO*	Arizona	34.3°N	116.2°W
UBO*	Utah	40.3°N	109.6°W
WMO*	Oklahoma	34.7°N	98.6°W

LHN was a small experimental array operated until Norsar was completed. ALQ, Albuquerque, New Mexico; BMO, Blue Mountains, Oregon; DUG, Dugway, Utah; EUR, Eureka, Nevada; KJN, Kajaani, Finland; LF4, Lasa F ring; NAO, Norsar; NUR, Nurmijarvi, Finland; TFO, Tonto Forest, Arizona; UBO, Uinta basin, Utah; WMO, Wichita Mountains, Oklahoma.
*Array stations.

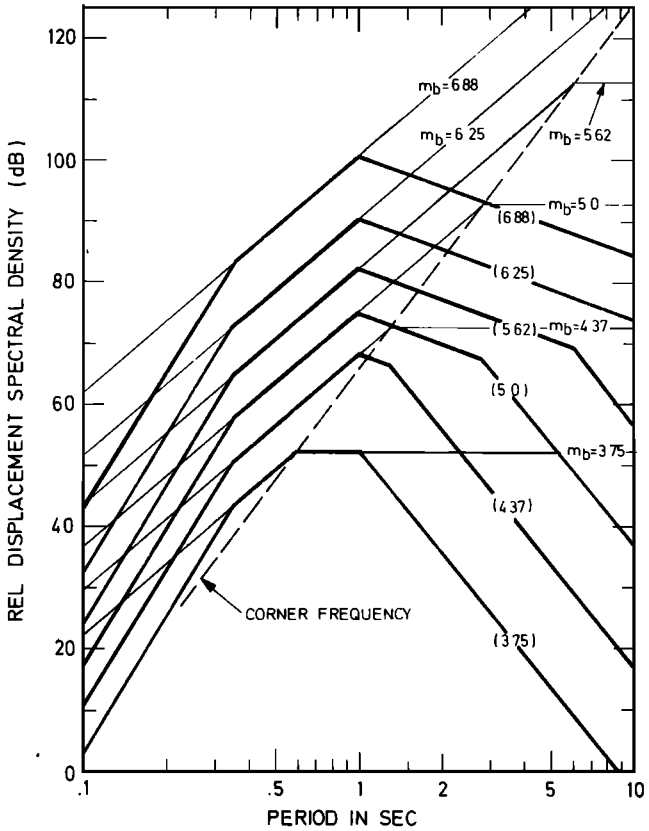

Fig. 9. The thin lines give the source factor of far-field spectral density from earthquakes with various M_s for *Aki*'s [1967] ω square model. The M_s-m_b relationship is $M_s = 1.59m_b + 3.97$, so that the m_b values scale differently from the original M_s; i.e., a m_b magnitude difference of 1.0 unit does not correspond to 20 dB in the figure. The thick lines show the seismic spectral density after it has been convolved with the WWSSN *SP-Z* instrument response.

event detectability is essentially a function of the signal-to-noise ratio, a positive or negative magnitude bias in the ISC or NOAA data may occur for sufficiently small events (see also Figure 6). On the other hand, our multivariate analysis showed that the ISC m_b estimate most likely was unbiased, and the reason might be that no really small earthquakes were used. In the case of Norsar-NOAA, the magnitude relationship seems to be more complex, but the minimum event magnitude in the data base was 3.60, whereas the corresponding value for ISC was 4.05. In short, both NOAA and ISC probably report reasonable event magnitude estimates for earthquakes having m_b values larger than, say, 4.0–4.2, whereas for very small events, systematic errors may occur owing to a severe limitation in the number of stations reporting *P* wave amplitudes, as is illustrated in Figure 5.

An original result presented in this paper is that the analysis of ISC data showed that station magnitude corrections could vary with event magnitude as shown in Figures 6 and 7 or in Tables 6 and 7. The same is probably true for the Norsar-NOAA relationship for some regions. Only in this particular case would propagation effects be considered (i.e., the joint effect of the frequency dependency of the crust–upper mantle *P* wave transfer function and seismic spectra scaling as a function of magnitude). Specifically, we have refrained from explaining the anomalies in terms of *Q* structures of the upper mantle, focusing effects in the vicinity of a downgoing slab [*Davies and Julian*, 1972], and focal mechanism variations. The reason is twofold. (1) Propagation effects of the above types are hardly separable. For example, the subarray amplitude pattern across Norsar is approximately stationary for a certain region but otherwise varies considerably even for small changes in epicentral distance and azimuth (see Table 1). (2) The cumulative propagation effect is likely to be multiplicative, not additive [*Bullen*, 1963], and thus the approximately log normal amplitude distribution is explained [*Ringdal et al.*, 1972; *Tartarski*, 1961].

Let us return to our problem, namely, that the magnitude measured at an individual station may vary, as a first approximation, linearly and differently with increasing earthquake magnitude. This result is explainable in terms of *Aki*'s [1967] scaling law model for seismic spectra, although the details on the spectral shape as a function of magnitude are somewhat hypothetical for frequencies above 0.1 Hz [*Aki*, 1972]. The crucial point is that small events emit relatively more high-frequency signal energy than large events. Only in this way can the observed station magnitude correction dependency on the m_b parameters be explained when the elastic and time invariant earth response to seismic waves is considered. Thus the spectral characteristics of short-period *P* waves may change with magnitude since the crust–upper mantle transfer function is most sensitive to higher signal frequencies and moreover varies considerably from one station site to another. A quantitative explanation of the station correction dependency on magnitude as the joint effect of spectral scaling and transfer functions is depicted in Figures 9 and 10. In Figure 9 the change in earthquake spectra with magnitude and modified by a World-Wide Standard Seismograph Network (WWSSN) Benioff *SP-Z* instrument is illustrated, the ω square model of *Aki* [1967] being used. Crust–upper mantle transfer functions for different Norsar subarrays were calculated by using the method of *Mack* [1969] and Japan earthquake data and are shown in Figure 10. From Figures 9 and 10 we conclude that changes, not necessarily linear, in the station correction term dm_{ij} are

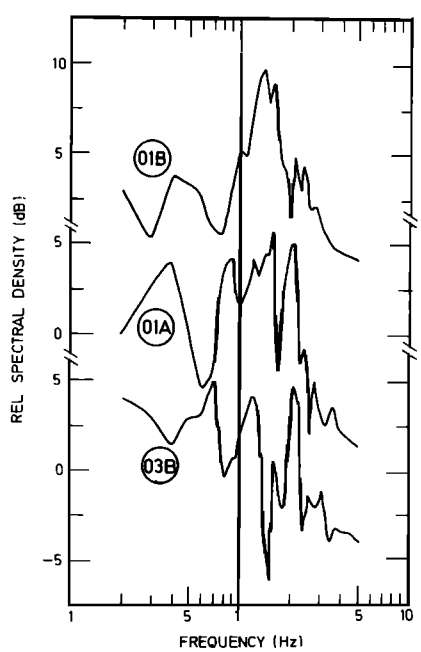

Fig. 10. Crust and upper mantle transfer function for a Japan event for some of the subbarrays at Norsar, calculated by the method of *Mack* [1969].

possible as a function of magnitude. A similar but more obvious case is that of seismometers having different amplitude response curves but identical locations, as demonstrated by *Marshall et al.* [1972].

An attempt to verify the above hypothesis was undertaken, but the results obtained were inconclusive. The starting point here was the subarray amplitude pattern across Norsar, which is based on data from events characterized by good signal-to-noise ratios. Using a large number of small Japanese events, we tried to check whether the array amplitude pattern remained fixed. Minor perturbations of the amplitude pattern were observed, but part of these seemed to be coupled to changes in epicenter locations. Moreover, for weak signals, computerized amplitude measurements are not very reliable owing to noise interference.

APPENDIX

The beam-forming process in a seismic array can be regarded as a summation of simple harmonic waves, where the signal losses are tied to random δt timing errors. Following *Steinberg* [1965], we may write

$$A_B(t) = \frac{1}{N} \sum_{k=1}^{N} A_k \cos \omega(t + \delta t_k) \qquad \text{(A1)}$$

where A_B is the array beam, N is the number of sensors, and A_k is the sensor amplitude.

Expanding the cosine term in (A1) will give

$$\sum_{k=1}^{N} A_k \cos \omega(t + \delta t_k) = \sum_{k=1}^{N} A_k \cos \omega t \cos (\omega \delta t_k) - \sum_{k=1}^{N} A_k \sin \omega t \sin \omega(\delta t_k) \qquad \text{(A2)}$$

The timing error δt_k can be considered randomly distributed at least for large N. Beam forming requires small timing errors in comparison with the period $\tau = 2\pi/\omega$ or $\delta t_k/\tau \ll 1$. Most terms in the second sum will consequently be small, and even for small N this sum can be omitted.

An approximation to (A1) is now

$$A_B(t) = \frac{1}{N} \sum_{k=1}^{N} A_k \cos (\omega \delta t_k) \cos (\omega t) \qquad \text{(A3)}$$

Both δt and A are independent variables having probability distributions $p(\delta t)$ and $p(A)$. Defining $F(A, \delta t) = A \cos (\omega \delta t)$, we proceed as follows:

$$\sum_{k=1}^{N} A_k \cos (\omega \delta t_k) \approx N\langle F(A, \delta t)\rangle = N \iint A \cos (\omega \delta t)\, p(\delta t)\, p(A)\, dA\, d(\delta t) = N \int Ap(A)\, dA \int \cos (\omega \delta t)\, p(\delta t)\, d(\delta t) \qquad \text{(A4)}$$

Now approximating the true mean value represented by the integrals with an average represented by sums, we obtain

$$\sum_{k=1}^{N} A_k \cos (\omega \delta t_k) = N \int Ap(A)\, dA \int \cos (\omega \delta t)\, p(\delta t)\, d(\delta t) \approx \frac{1}{N} \sum_{k=1}^{N} A_k \sum_{k=1}^{N} \cos (\omega \delta t_k) \qquad \text{(A5)}$$

or denoting

$$C_L = \frac{1}{N} \sum_{k=1}^{N} \cos (\omega \delta t_k)$$

the array beam is

$$A_B(t) = \frac{C_L}{N} \sum_{k=1}^{N} A_k \cos (\omega t) \qquad \text{(A6)}$$

Acknowledgments. Director E. P. Arnold, International Seismological Centre, Edinburgh, provided us with tape copies of ISC data files, and this service is much appreciated. We are indebted to A. Christoffersson for his most helpful suggestions in the multivariate ISC data analysis and hypothesis test, and we also wish to thank D. Doornbos for critically reading the manuscript. Until June 30, 1973, the Norsar project was sponsored by the United States of America under the overall direction of the Advanced Research Projects Agency and the technical management of Electronic Systems Division, Air Force Systems Command, through contract F19628-70-C-0283 with the Royal Norwegian Council for Scientific and Industrial Research. Since July 1, 1973, the project has been sponsored by the U.S. Air Force and monitored by the European Office of Aerospace Research and the Air Force Office of Scientific Research, Air Force Systems Command, under contract F44620-74-C-0001 with the Royal Norwegian Council for Scientific and Industrial Research.

REFERENCES

Aki, K., Scaling law of seismic spectrum, *J. Geophys. Res., 72,* 1217–1231, 1967.

Aki, K., Scaling law of earthquake source time function, *Geophys. J. Roy. Astron. Soc., 31,* 3–25, 1972.

Aki, K., Scattering of *P* waves under the Montana Lasa, *J. Geophys. Res., 78,* 1334–1346, 1973.

Anderson, T. W., *An Introduction to Multivariate Statistical Analysis,* chap. 11, pp. 272–287, John Wiley, New York, 1958.

Basham, P. W., and R. B. Horner, Seismic magnitudes of underground nuclear explosions, *Bull. Seismol. Soc. Amer., 63,* 105–132, 1973.

Båth, M., *Handbook on Earthquake Magnitude Determinations,* Seismological Institute, Uppsala, Sweden, 1969.

Berteussen, K. A., and E. S. Husebye, Predicted and observed seismic event detectability of the Norsar array, *Tech. Rep. 42,* 12 pp., Norg. Tek. Naturvitensk. Forskning./Norsar, Kjeller, Norway, 1972.

Bullen, K. E., *An Introduction to the Theory of Seismology,* chap. 8, pp. 125–136, Cambridge University Press, London, 1963.

Bungum, H., and E. S. Husebye, Analysis of the operational capabilities for detection and location of seismic events at Norsar, *Bull. Seismol. Soc. Amer., 64,* in press, 1974.

Bungum, H., E. S. Husebye, and F. Ringdal, The Norsar array and preliminary results of data analysis, *Geophys. J. Roy. Astron. Soc., 25,* 115–126, 1971.

Capon, J., Characterization of crust and upper mantle structure under Lasa as a random medium, *Bull. Seismol. Soc. Amer., 64,* 235–266, 1974.

Davies, D. (Rapporteur), *Seismic Methods for Monitoring Underground Nuclear Explosions,* pp. 59–68, Swedish Institute for Peace and Conflict Research, Stockholm, 1968.

Davies, D., and B. R. Julian, A study of short period *P*-wave signals from Longshot, *Geophys. J. Roy. Astron. Soc., 29,* 185–202, 1972.

Evernden, J. F., Magnitude determination at regional and near-regional distances in the United States, *Bull. Seismol. Soc. Amer., 57,* 591–639, 1967.

Gutenberg, B., Amplitudes of surface waves and magnitudes of shallow earthquakes, *Bull. Seismol. Soc. Amer., 35,* 3–12, 1945.

Gutenberg, B., and C. F. Richter, Magnitude and energy of earthquakes, *Ann. Geofis., 9,* 1–15, 1956.

IBM, *Third Quart. Tech. Rep. ESD-TR-68-149,* 179 pp., Fed. Syst. Div., Gaithersburg, Md., 1967.

Karnik, V., *Seismicity of the European Area,* sect. 2.35, pp. 34–50, D. Reidel, Dordrecht, Netherlands, 1969.

Lacoss, R. R., and G. T. Kuster, Processing a partially coherent large seismic array for discrimination, *Tech. Note EST-TR-70-353,* 47 pp., Lincoln Lab., Mass. Inst. of Technol., Cambridge, 1970.

Mack, H., Nature of short-period *P* wave signal variations at Lasa, *J. Geophys. Res., 74,* 3161–3170, 1969.

Marshall, P. D., R. F. Burch, and A. Douglas, How and why to record broad band seismic signals, *Nature, 239,* 154–155, 1972.

Morrison, D. R., *Multivariate Statistical Methods,* p. 250, McGraw-Hill, New York, 1967.

Noponen, I., E. S. Husebye, and D. Rieber-Mohn, Extraction of *P*-wave spectra using the Norsar array, *Proc. Seminar Seismol Seismic Arrays,* 85–101, 1972.

Ringdal, F., E. S. Husebye, and A. Dahle, Event detection problems using a partially coherent seismic array, *Tech. Rep. 45,* 23 pp., Norg. Tek. Naturvitensk. Forskning./Norsar, Kjeller, Norway, 1972.

Siegel, S., *Nonparametric Statistics for the Behavioral Sciences,* int. stud. ed., pp. 229–239, McGraw-Hill, New York, 1956.

Steinberg, B. D., Large aperture teleseismic array theory, in *Report of First Lasa Systems Evaluation Conference in Billings, Montana,* pp. 140–154, Advanced Research Projects Agency, Washington, D. C., 1965.

Tartarski, V. I., *Wave Propagation in a Turbulent Medium,* translated by R. A. Silverman, pp. 208–209, McGraw-Hill, New York, 1961.

(Received August 6, 1973;
revised March 27, 1974.)